

Lead monoxide α -PbO: electronic properties and point defect formation.

J. Berashevich ^{‡,1} O. Semeniuk,^{1,2} O. Rubel,^{1,2} J.A. Rowlands,¹ and A. Reznik^{1,2}

¹Thunder Bay Regional Research Institute, 290 Munro St., Thunder Bay, ON, P7B 5E1, Canada

²Department of Physics, Lakehead University, 955 Oliver Road, Thunder Bay, ON, P7B 5E1

The electronic properties of polycrystalline lead oxide consisting of a network of single-crystalline α -PbO platelets and the formation of the native point defects in α -PbO crystal lattice are studied using first principles calculations. The α -PbO lattice consists of coupled layers interaction between which is too low to produce high efficiency interlayer charge transfer. In practice, the polycrystalline nature of α -PbO causes the formation of lattice defects in such a high concentration that defect-related conductivity becomes the dominant factor in the interlayer charge transition. We found that the formation energy for the O vacancies is low, such vacancies are occupied by two electrons in the zero charge state and tend to initiate the ionization interactions with the Pb vacancies. The vacancies introduce localized states in the band gap which can affect charge transport. The O vacancy forms a defect state at 1.03 eV above the valence band which can act as a deep trap for electrons, while the Pb vacancy forms a shallow trap for holes located just 0.1 eV above the valence band. Charge de-trapping from O vacancies can be accounted for the experimentally found dark current decay in ITO/PbO/Au structures.

I. INTRODUCTION

Polycrystalline lead oxide (PbO) is one of the most promising photoconductive materials for use as a x-ray-to-charge transducer in direct conversion x-ray detectors [2]. Since the direct conversion detection scheme offers a number of advantages over the indirect conversion, [3], photoconductive materials for x-ray imaging have recently attracted much interest. The four most important criteria when potential x-ray photoconductors are considered include: (1) high conversion gain; (2) high x-ray absorption efficiency; (3) compatibility with large area detector technology and (4) good photoconductive properties. PbO satisfies the first three criteria. However, thick PbO does not show adequate transport properties and this results in poor temporal characteristics (signal propagation/delay time) [2, 4]. This is the primary issue in the development of PbO in x-ray medical imaging detectors.

For use in x-ray detectors, photoconductive layers are deposited directly over an imaging matrix. When PbO layer is deposited in the evaporation process, it condenses in very thin platelets a few micrometers in size which have a porosity of around 50% [2]. On the mesoscopic scale a single platelet is a collection of the stacked PbO layers [5] (Fig. 1). It is expected that a layered structure will result in anisotropy in the transport properties and inter-platelets and/or interlayer charge transfer will limit the overall charge mobility.

Another common reason for the low charge drift mobility in polycrystalline compounds that must be considered in PbO is charge carrier trapping. Traps capture the photogenerated carriers or act as the scattering or recombination centers [6]. Generally, the effect of the carrier trapping on the transport properties depends on the trap concentration. The process of carrier de-trapping from shallow traps is fast in comparison to the deep traps which tend to hold the carriers longer, thereby significantly impairing the temporal characteristics of the ma-

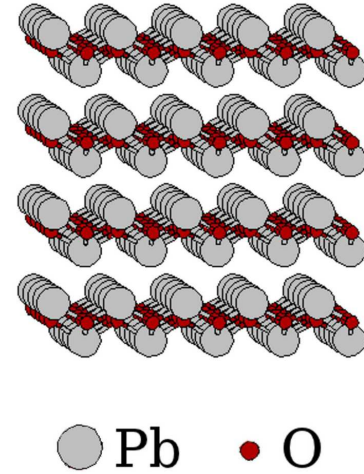


FIG. 1: The crystal structure of the tetragonal α -PbO of the space group 129P4/nmm.

terial. For x-ray application, the worst situation is when the carriers de-trapping becomes longer than the collection time of the X-ray signal and as such the de-trapped carriers contribute to the appearance of image artifacts known as 'ghosting' [7]. This limits the application of the PbO-based detectors in real-time imaging procedures.

Thermally deposited PbO has an oxygen deficiency [8–10]. Although the effect of the O vacancies on transport in PbO is not clearly understood, it was found that thermal annealing in pure oxygen increases the electrical conductivity that can be attributed to the reduction of the oxygen vacancy concentration [8]. Unfortunately, high-temperature annealing is not practical for PbO layers deposited over an imaging matrix. Therefore, comprehensive studies of PbO structure and defect formation in thermally evaporated PbO layers are needed to improve the temporal characteristics of the PbO compound. A

growth process must be developed to reduce the trap concentration and ultimately to improve the performance of PbO for real time x-ray detector applications. We started our investigations by modelling α -PbO crystal lattice, revealing the crystal structure parameters and verifying them with available theoretical and experimental data. Due to limitation of the software used, the dispersive interactions have been neglected in our studies. The effect of this assumption on results is discussed in Sec. II. Further, the vacancies have been induced into the lattice of α -PbO and defect formation energies, energetic location of the defects within the band gap and potential of their transition to the charged states have been investigated. In order to show the consistency of our results with the experimental data, we completed our work with measurements of the dark current on the ITO/PbO/Au samples with an analysis of the trap participation in the charge transport process.

II. CALCULATION TECHNIQUE AND EXPERIMENT

A. Calculation technique

In our study we applied the density functional theory (DFT) available in the Wien2k package [11] which utilizes the full-potential augmented plane-wave method. All calculations of the electronic structure were performed with the Perdew-Burke-Ernzerhof parametrization [12] of the generalized gradient approximation (GGA) to DFT.

Calculations of the formation energy of defects (the cohesive properties) with DFT methods require attention to many parameters and calculations with high precision have to be implemented. Applying the appropriate energy cut off to separate the core and valence states we treated $5p$, $5d$, $6s$ and $6p$ electrons of Pb atoms and $2s$ and $2p$ electrons of O atoms as valence electrons. The inclusion of the $5d$ states of Pb atom in the valence states (not in the core states) is required to introduce a proper description of bonding and orbital hybridization of Pb atoms with O atoms. Indeed, the orbital energy of the $5d$ electrons in Pb atoms and $2p$ electrons in O atom are located in the same energy range [13]. There is one more parameter needing special attention when the cohesive properties are studied, the so-called RK_{max} parameter, which is the product of the atomic sphere radius and the plane-wave cutoff in k -space. In our calculation it was assigned as 8. The Brillouin zone of a primitive cell for most of the calculations was set to a $11 \times 11 \times 8$ Monkhorst-Pack mesh. When the supercell procedure was used, the size of the Monkhorst-Pack mesh was adjusted to the size of the supercell, i.e. the mesh was appropriately reduced as the supercell was enlarged. The calculations of the formation energy of the native point defects have been done with the sufficiently large supercell of 108-atom size ($3 \times 3 \times 3$ array of the primitive unit cells) and $4 \times 4 \times 3$ Monkhorst-Pack mesh.

The optimization procedure for the α -PbO lattice was performed based on minimization of the forces [14] and it provided us with the following lattice parameters: lattice constants $a_0 = 4.06 \text{ \AA}$ (within the layer) and $c_0 = 5.51 \text{ \AA}$ (inter-layer distance) with the ratio $c_0/a_0 = 1.357$ and the Pb-O bond length of 2.35 \AA . The achieved magnitude for a_0 is identical to the value obtained with GGA in Ref. [15] and is in excellent agreement with the experimental value of 3.96 \AA obtained in Ref. [5]. The calculated length of Pb-O bond is in agreement with other theoretical studies [16] and correlates well with an experimental value of 2.32 \AA [5]. The second lattice parameter c_0 agrees very well with GGA calculations performed in Ref. [16, 17] but is larger than the experimentally determined value of 5.07 \AA [15].

The mismatch in lattice parameter c_0 occurs due to limitations of GGA functional which does not include into account the dispersive interactions. In attempt to compensate for this limitation, we have used the experimental value of the lattice parameter $c_0 = 5.07 \text{ \AA}$ [15] that induces a reduction in layer separation. As a result, an increase in the interlayer interaction strength has contributed into a raise of the layers binding energy from 0.013 eV/atom to 0.016 eV/atom being surprisingly small (calculated as the difference in the total energy between the systems of a single layer and two layers of α -PbO). However, it has caused significant suppression in the band gap size. If for the optimized lattice constant $c_0 = 5.51 \text{ \AA}$ the indirect gap $\Gamma - M^*$ is 1.8 eV [18] which is in good agreement with experimentally found optical gap of $1.9 \pm 0.1 \text{ eV}$ [19], with implementation of the lattice parameter $c_0 = 5.07 \text{ \AA}$ [15], the gap shrinks by 0.22 eV . The important distinction of the α -PbO crystal structure is that the layers are held together by the weak orbital overlap of the $6s^2$ lone pairs [13] while reduction of c_0 leads to an overestimation of the interlayer overlap of these orbitals by GGA. Since the indirect gap is defined by strength of the interlayer interactions, it decreases with c_0 suppression [18]. Similar was observed for SnO which has the same lattice type as α -PbO (129P4/nmm space group) for which inclusion of the dispersive interactions while correcting the lattice parameters caused unreasonable reduction in the band gap sizes E_G [20]. However, the formation energies of vacancies did not show strong dependence on the lattice parameter c_0 . The vacancy states are localized entirely within the single layer, such as their formation energy is affected strongly only by the lattice constant a_0 and length of the Pb-O bond, but contribution of the interlayer interactions defined by c_0 is negligibly small. For the purposes of this work, the large discrepancy in the band gap size makes it difficult to define correctly an appearance of defects inside the band gap. Therefore, in order to achieve the meaningful results on both, location of the defect states inside the band gap and their formation energy, we found more justified to use the optimized lattice constant $c_0 = 5.51 \text{ \AA}$ (see Sec. III).

The value of the interlayer interactions in order of 0.013

eV/atom (0.016 eV/atom for $c_0=5.07 \text{ \AA}$) is lower than thermal energy at room temperature $kT \simeq 0.026 \text{ eV}$ and much lower than in most other solid state materials. For example, in graphite which consists of stacked graphene layers, the interlayer interactions were found to be 0.052 eV/atom [21]. The extremely low magnitude of interactions in α -PbO is similar to the inter-molecular interactions in π -conjugate organic systems [22]. For π -conjugate organic systems the low interlayer interaction is the primary reason for the extremely low carrier mobility. Since in PbO the interlayer interaction is half of kT at room temperature, we anticipate that the interlayer electron transport in α -PbO by all potential transport mechanisms would be insufficient, meaning that electron mobility in this direction is extremely low. This statement is supported by the almost dispersionless valence bands observed in the band diagram of α -PbO [13].

B. Experimental details

Thick (40 μm) PbO layers were deposited on ITO-covered Corning glass substrates by thermal evaporation of the PbO powder (purity 99.9999 %) in a vacuum of 0.2 Pa under additional molecular oxygen flow. The growth rate was 1 $\mu\text{m}/\text{min}$. The substrate was kept at 120° C to suppress the growth of β -PbO [2] (grown PbO layers may contain a trace of other lead-compounds) and to achieve good adhesion to the substrate. Subsequently, gold contacts were deposited through the contact mask by a sputtering technique. The resulting ITO/PbO/Au structures were biased to different electric fields (ITO was negatively biased) and time dependence of the dark current density was measured automatically every second for 50 minutes.

III. RESULTS AND DISCUSSION

A. Native point defects

As it was mentioned above, in practice thermally grown polycrystalline α -PbO contains large amount of the O vacancies [8–10]. Therefore, in this work we consider the formation of the native point defects (i.e. O or Pb vacancies) assuming that no impurities responsible for formation of other type of defects are present. This assumption is quite reasonable when PbO is grown in vacuum employing only molecular oxygen flow. We applied a supercell approach in which the larger is the supercell size, the smaller is the interaction between the repeated units (neighbouring supercells each containing a defect). A truly isolated defect should show the dispersion-less flat band on the band diagram which was indeed received with a supercell of 108-atom size ($3 \times 3 \times 3$ array).

We examined the formation of vacancy defect by removing one of the corresponding atoms from the α -PbO lattice and then optimized its geometry with respect to

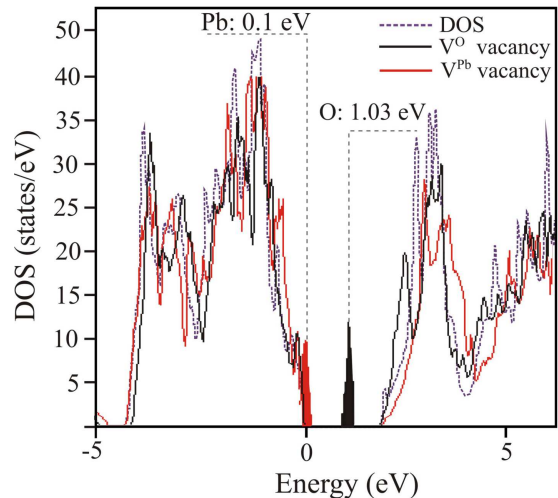


FIG. 2: Colour on-line. Density of states calculated for defect free α -PbO (dashed line) and the same system with defects (solid lines): DOS for the O vacancy is shown by red solid line while for the Pb vacancy it is marked by a black line. The energetic location of the vacancy states inside the band gap relatively the top of the valence band is $E_D(V^O)=1.03 \text{ eV}$ and $E_D(V^{Pb})=0.01 \text{ eV}$ for the O vacancy and, the Pb vacancy, respectively.

the internal degrees of freedom. As a single defect is induced, the lattice rearrangement around the defect site occurs. Within the α -PbO lattice, the layer of O atoms are tightly sandwiched between Pb atoms (see Fig. 1), i.e. the Pb atoms are located on the side of the layers holding the skeleton of each layer. Therefore, removal of the Pb atom from the lattice induces a significant lattice rearrangement, while in the case the O atom of small atomic radius is removed, the distortion of the lattice is minimal. Thus, removal of Pb atom (V^{Pb}) initiates the enlargement of the distance between O atoms which were bonded to Pb site, and each O atom moves apart from the defect site by 0.22 \AA due to a repulsion felt by the O ions. In contrast, the lattice modification induced by the O vacancy is almost unnoticeable: Pb atoms move only by 0.07 \AA toward the vacancy site.

We show in Fig. 2 an alteration in the density of states (DOS) as defects are induced into the α -PbO lattice. Insertion of either O or Pb vacancy creates the defect level inside the band gap and the electronic density for the defect state is strongly localized in both cases. The electron density distribution outside the band gap is not significantly affected by the presence of defects since only O: $2p^4$ and Pb: $6p^2$ electrons participate in formation of the Pb-O bond (these states are located close to the band gap edges). Our results indicate that O vacancy (V^O) forms the defect level near the midgap. The energetic location of this defect level is $E_D(V^O)=1.03 \text{ eV}$ above the top of the valence band E_V as shown in Fig. 2. The O vacancy in its uncharged state is already filled with two electrons. Because O atom forms 4 bonds with nearest

Pb atoms in the α -PbO lattice, a removal of a single O atom leaves 0.5 unbounded electrons on each Pb atom that overall results in occupation of this defect level by two electrons. The Pb vacancy (V^{Pb}) induces the defect energetically located close to the top of the valence band with $E_D(V^{\text{Pb}})=0.1$ eV and this vacancy is not filled with electrons.

B. The formation energy of the vacancies

The formation energy of a vacancy is an important parameter as it determines how likely a vacancy will be generated in the compound under given growth conditions. The formation energy is mainly defined by several parameters: (i) type of the crystal structure as energy required to remove an atom from the crystal structure depends on the strength of the electronic interactions within the lattice, (ii) the final state of the removed species, (iii) the characteristics of the environment, i.e. growth conditions.

The formation energy of a defect D in charge state q can be defined as [25]:

$$\Delta E^f(D) = E_{tot}(D^q) - E_{tot}(S) + \sum_i n_i \mu_i + q(E_F + E_V + \Delta V) \quad (1)$$

where $E_{tot}(D^q)$ and $E_{tot}(S)$ are the total energy of the system containing the single defect and defect-free system, respectively. n_i indicates a number of i -atoms removed while μ_i is the chemical potential of those atoms. $(E_F + E_V)$ is the position of the Fermi level relative to the valence band maximum (E_V). q defines the charge of the state (+2/+1/0/-1/-2). For the charged point defects, the position of the valence band E_V has to be corrected with ΔV calculated through alignment of the reference potential in defective supercell with that in bulk α -PbO (for details see Ref. [25]). The formation energy of the defects has been also corrected with so-called band gap error ΔE_G [23] which is defined as a difference between the direct band gap $\Gamma\text{-}\Gamma^* = 1.94$ eV and the experimental optical band gap of 1.9 eV [19]. In this particular case, the contribution of $\Delta E_G = -0.04$ eV into the formation energy is minor because of good agreement of the theoretical value and experimental data (a value of the corrected band gap of supercell [23] is 1.89 eV). The formation energy has been increased by this band gap correction $m\Delta E_G$, where m is the number of the electron at the defect site.

The chemical potentials are defined as following $\mu_i = E_{tot}(i) + \mu_i^*$, where $\mu_i^* = \mu_i^0 + kT \cdot \ln(p/p^0)$ is the part related to real growth conditions: the partial pressure p and temperature T (μ_i^0 is an alteration to the chemical potential induced by change of temperature from 0 to T under the standard pressure p^0). However, not willing to speculate on the Pb and O partial pressures used during deposition, we consider the extreme cases, i.e. the Pb-rich or O-rich growth conditions ($\mu_{(\text{Pb})} = \mu_{(\text{Pb})[\text{bulk}]}$ and

$\mu_{(\text{O})[\text{O}_2]}$, respectively) as it was suggested in Refs. [20, 23, 25, 27]. The chemical potentials for the extreme cases can be evaluated through the standard enthalpy of formation $\Delta_f H^0(\text{PbO})$ as [25]:

$$E_{tot}(\text{PbO}) = \mu_{(\text{Pb})[\text{bulk}]} + \mu_{(\text{O})[\text{O}_2]} + \Delta_f H^0(\text{PbO}) \quad (2)$$

where $E_{tot}(\text{PbO})$ is the total energy of the product; $\mu_{(\text{Pb})[\text{bulk}]}$ and $\mu_{(\text{O})[\text{O}_2]}$ are the chemical potentials of bulk Pb and O_2 molecule, respectively. Therefore, $\Delta_f H^0(\text{PbO})$ is an important parameter in definition of the chemical potentials. In the calculation of $\Delta_f H^0$ for oxides the main discrepancy between the theoretical and experimental data is known to come from the binding energy of the O_2 molecule ($\Delta_f H^0(\text{O}_2)$) used in definition of the chemical potential $\mu_{(\text{O})[\text{O}_2]} = \frac{1}{2}(2E_{tot}(\text{O}) + \Delta_f H^0(\text{O}_2) + \mu_{(\text{O}_2)}^*)$ [26–28]. To disregard this error in our calculations we used the experimental value of $\Delta_f H^0(\text{O}_2) = -5.23$ eV [29] (best theoretical estimation is $\Delta_f H^0(\text{O}_2) = -6.01$ eV [26]). With that assumption we obtained $\Delta_f H^0(\text{PbO}) = -2.92$ eV per Pb-O pair which is in appropriate agreement with the experimental value of $\Delta_f H^0(\text{crystal } \alpha\text{-PbO}) = -2.29$ eV [24].

It is known that regardless the deposition techniques used, the PbO layers are not stoichiometric and has deficit of oxygen [8–10]. Hence, we consider the Pb-rich/O-poor conditions for which the O-poor limit has been assigned to $\mu_{(\text{O})}^* = \Delta_f H^0(\text{PbO})$ [23] ($\mu_{(\text{O})}^* = -2.92$ eV), while Pb-rich limit has been found from relation $\Delta_f H^0(\text{PbO}) = \mu_{(\text{Pb})}^* + \mu_{(\text{O})}^*$ ($\mu_{(\text{Pb})}^* = 0$ eV). The formation energy of the defects $\Delta E^f(D)$ for V^{O} and V^{Pb} for the different charge states calculated with help of Eq. 1 are presented in Fig. 3.

The O vacancy in its neutral state is occupied by two electrons. If the O vacancy drops electron (1+ charged states), its formation energy is reduced. The Pb vacancy in its uncharged state is empty $V^{\text{Pb}(0)}$ and its formation energy is comparably high, but is lowered if vacancy accepts electrons (1–/2– charged states). Therefore, both the O and Pb vacancies (V^{O} and V^{Pb}) intend to appear in the opposite charged states. The neutral O vacancy would prefer to give away one electron to reduce its formation energy. To conserve the electroneutrality of material there are only the Pb vacancies that can accept electrons under the equilibrium conditions. This makes the Pb vacancy a compensation center for the O vacancy. The considered mechanisms of the charge exchange between vacancies are presented Fig. 4 (a) and (b). In case of thermodynamic equilibrium, when formation energies for both types of vacancies are equal and, therefore, their concentrations are equal as well, vacancies would become doubly ionized ($V^{\text{Pb}(2-)}$ and $V^{\text{O}(2+)}$) utilizing the mechanism of the electron exchange as presented in Fig. 4 (a).

However, for the Pb-rich/O-poor limit considered in present work the formation energies of the vacancies are different from the thermodynamic equilibrium (see Fig. 3). As seen in Fig. 3, the formation energy of the O vacancy is much lower than the Pb vacancy. This

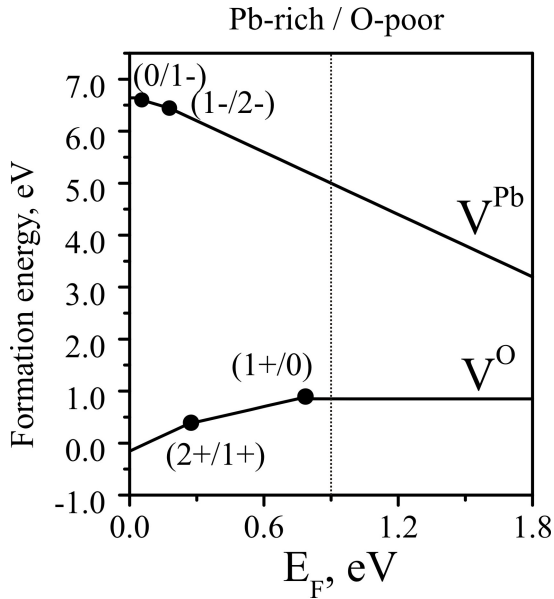


FIG. 3: The formation energy of the defects $\Delta E^f(D)$ for V^O and V^{Pb} for Pb-rich/O-poor limit. The charge states for which added electron or hole remains localized on the vacancy site are shown ($1+/2+$ states for the V^O vacancy and $2-/1-$ states for the V^{Pb} vacancy).

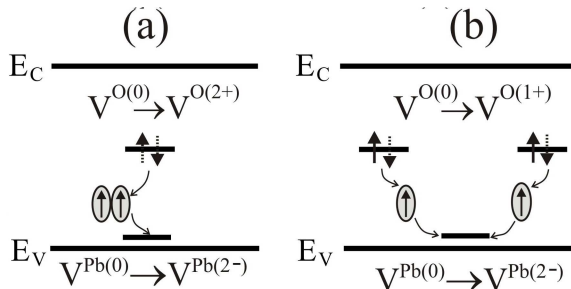


FIG. 4: Schemes showing the mechanisms of ionization of the neutral vacancies through the electron exchange (V^{Pb} accepts two or single electron occupying the V^O vacancy).

presumes much higher concentration of the O vacancies so that they will be only partially compensated by the Pb vacancies. Based on achieved magnitude of the formation energies we expect the Pb vacancies to appear preferably in their $(2-)$ states while the O vacancies to be formed in the different charged states, $(0)/(1+)$. In this case, ionization of the Pb vacancy to the $V^{Pb(2-)}$ state can occur with participation of two O vacancies such as each $V^{O(0)}$ donates single electron becoming ionized only to the $V^{O(1+)}$ state as presented in Fig. 4 (b). The O vacancies in the $V^{O(1+)}$ state are still occupied by one electron, and the larger the difference in O/Pb vacancy concentration, the larger amount of the non-compensated O vacancies. This behaviour helps in understanding of the experimentally observed n -conductivity of PbO [8–10]. Both neutral and singly charged O vacancies ($V^{O(0)}$ and $V^{O(1+)}$) act as n -type donor. Moreover, in this case,

a pinning of the Fermi level position slightly above the midgap (0.95 eV below the conduction band) observed experimentally [31] can be assigned to n -type doping induced by the O vacancies. Previously, the pinning was associated with the surface states at the crystallites boundaries but nature of those states was unknown [31]. A remarkable agreement between the Fermi level position predicted in Ref.[31] and position of the O vacancy states found here (see Fig. 2) suggests that the Fermi level is stabilized by the presence of the O vacancies.

Therefore, we anticipate that the O vacancies would affect the transport and photogeneration in lead oxide more significantly than the Pb vacancies. Indeed, shallow traps for holes created by the ionized Pb vacancies might slightly reduce the hole mobility which is already low due to the extremely heavy holes [18], but much deeper O vacancies when they are ionized (see Fig. 2) would not only slow down the electron propagation in the conduction band through trapping, but can additionally act as the recombination centers. Therefore, because a contribution of the deep traps in the charge transport is known to impair significantly the current decay [32, 33], the temporal behaviour of the dark conductivity can be used to confirm a presence of the O vacancies.

C. Dark current kinetics

The dark current kinetics is a sensitive measure of the electronic properties of a material and is used here to describe the effect of point defects on the conductivity in PbO layers. The results of time dependence of the dark current density for selected biases are shown in Fig. 5. As it is seen from Fig. 5, after bias voltages are applied dark current decays slowly reaching a steady state value after about 250 minutes. The steady-state current density depends on electric field and increases by a factor of 2 when bias is increased from 3 to 7 $V/\mu m$. Similar behaviour of the dark current was observed by Mahmood and Kabir in amorphous selenium (a-Se) multilayer $n-i-p$ structures [32] and by Street in hydrogenated amorphous silicon (a-Si:H) $p-i-n$ structures [33, 34]. Mahmood and Kabir explain dark current decay in a-Se multilayer structure by carrier trapping within comparatively thick (few μm [35]) n - and p - layers which induces screening of the electric field at the metal/ n - or p -layer interfaces. The subsequent redistribution of the electric field suppresses carrier injection from metal contacts and reduces the dark current which is mainly controlled by the injection.

An alternative model is suggested by Street who explains similar dark current kinetics by depletion of charge from the bulk of i -layer assuming that dark current is controlled by thermal generation from defects states in the gap. As traps are depleting, the quasi Fermi level moves toward the midgap and the thermal generation current decreases [33]. As PbO samples studied here are uniform, we have to assume that the electric field is also

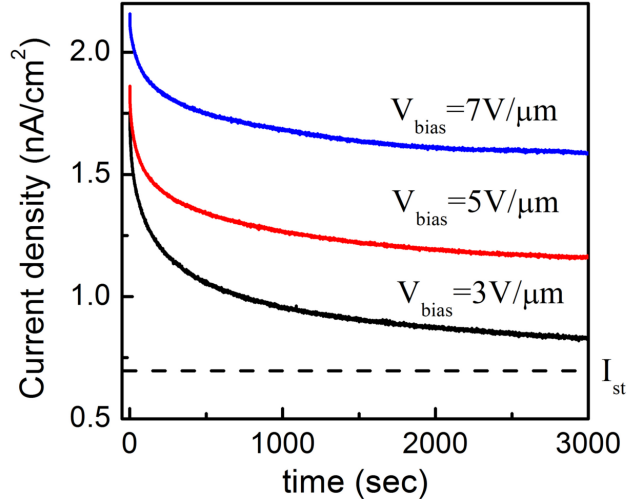


FIG. 5: Colour on-line. The time dependence of the dark current density for the different bias applied. I_{st} is the steady state current which is reached at 1.5×10^4 sec.

uniform across the layer (neglecting thin pre-contact areas). Therefore, the model developed by Street is more applicable in our case. Neglecting charge carrier injection under the applied low biases, we can assume that the thermal generation current arises from the excitation from the O vacancies occupied by electrons to the conduction band. Hence the dark current decay can be described by the time dependent quasi Fermi level position as is was suggested in Ref. [33]. Without speculating on the degree of compensation in our layers we assume that quasi Fermi level is initially located at 1.03 eV from the valence band, i.e. the activation energy is 0.77 eV. After an electric field is applied, the occupancy of the O vacancies changes as electrons are emitted to the conduction band and the quasi Fermi level shifts toward the midgap. Once traps are fully depleted quasi Fermi level approaches the equilibrium Fermi level and the thermal generated current saturates at electric field dependent steady-state value.

Although at that point we provide just qualitative analysis of dark current kinetics in PbO layers, it allows us to link defects (namely, the O vacancies) with transport properties in this material. It has to be mentioned that steady-state dark current is extremely low (and much lower than in a-Se [32]) that is very encouraging for the application of PbO layers in direct conversion medical x-ray imaging detectors [36].

IV. CONCLUSION

First-principles density-functional calculations were used to calculate the electronic properties of polycrystalline α -PbO and the formation of native point defects (namely, O and Pb vacancies) in this material. It was found that the O vacancies induce very deep donor level close to the midgap at 1.03 eV above the valence band. In contrast, the Pb vacancies create shallow defect level at just 0.1 eV above the valence band which acts as acceptor. Under applied bias the ionized O vacancies in PbO would act as the deep traps and recombination centers for the electrons in the conduction band, while the Pb vacancies are the shallow traps for holes in the valence band.

The formation energies of the defects in their neutral charge states are comparatively small: 0.85 eV for the O vacancy and 6.64 eV for the Pb vacancy (E_F is assigned to the midgap and the Pb-rich/O-poor growth conditions are considered) and are further reduced if a vacancy appears in its energetically favourable charged state. For example, for the doubly ionized (2-) Pb vacancy the formation energy is reduced to 4.99 eV. The electron exchange between vacancies initiates ionization of the vacancies, but for Pb-rich/O-poor growth conditions when concentration of the vacancies is not balanced, most of the O vacancies remains unionized, i.e. in their (0) uncharged state or (1+) charged state in which the O vacancies are occupied with electrons.

The presence of defects and differential trapping of electrons and holes were predicted by others to explain space charge limited photoconductivity in PbO [4] and to model x-ray sensitivity, modulation transfer function (MTF) and detective quantum efficiency (DQE) of the PbO x-ray detector [6]. The results presented here agree well with these studies and provide insight into the nature of defects in PbO clarifying their electronic and charge states and explaining why vacancies exist in high concentration in thermally evaporated PbO layers. Moreover, our own experimental results on time dependence of the dark current density suggest that this is the field dependent occupancy of O vacancies that governs the dark current kinetics. Thus, the O vacancies are occupied with electrons and because these centers are located close to the midgap of PbO, a process of detrapping of the vacancies is slow thus impairing the temporal characteristics of compound.

Since O vacancies play more essential role in the transport properties of PbO layers, material science solutions must be found to improve PbO layers deposition techniques in order to suppress their appearance. Methods to consider include thermal evaporation with optional low energy O ion bombardment or passivation of vacancies by post-growth annealing in oxygen atmosphere.

Since O vacancies play more essential role in the transport properties of PbO layers, material science solutions must be found to improve PbO layers deposition techniques in order to suppress their appearance. Methods to consider include thermal evaporation with optional low energy O ion bombardment or passivation of vacancies by post-growth annealing in oxygen atmosphere.

Acknowledgement

Authors are thankful to Dr. Matthias Simon (X-ray Imaging Systems, Philips Research) for numerous stimulating discussions and Giovanni DeCrescenzo for technical support in conducting the dark-current measure-

ments. Financial support of Ontario Research Fund- Research Excellence program is highly acknowledged.

-
- [‡] Electronic mail: berashej@tbh.net
- [2] Simon M, Ford R A, Franklin A R, Grabowski S P, Menser B, Much G, Nascetti A, Overdick M, Powell M J and Wiechert D U 2005 *IEEE Transactions on Nuclear Science* **52**, 2035.
- [3] Kasap S, Frey J B, Belev G, Tousignant O, Mani H, Greenspan J, Laperriere L, Bubon O, Reznik A, De-Crescenzo G, Karim K S and Rowlands J A 2011 *Sensors* **11** 5112.
- [4] Hughes R C and Sokel R J 1981 *J. Appl. Phys.* **52** 6743.
- [5] Leciejewicz J 1961 *Acta Cryst.* **14** 1304.
- [6] Kabir M Z 2008 *J. Appl. Phys.* **104** 074506.
- [7] Rau A W, Bakueva L and Rowlands J A 2005 *Med. Phys.* **32** 3160.
- [8] Hwang O, Kim S, Suh J, Cho S and Kim K 2011 *Nuclear Instruments and Methods in Physics Research A* **633** S69.
- [9] Bigelow J E and Haq K E 1962 *J. Appl. Phys.* **33** 2980.
- [10] Scanlon D O, Kehoe A B, Watson G W, Jones M O, David W I F, Payne D J, Egdell R G, Edwards P P and Walsh A 2011 *Phys. Rev. Lett.* **107** 246402.
- [11] Blaha P, Schwarz K, Madsen G K H, Kvasnicka D and Luitz J *Wien2k: An Augmented Plane Wave + Local Orbitals Program for Calculating Crystal Properties: Karlheinz Schwarz*, (Techn. Universität Wien, Austria, 2001)
- [12] Perdew J P, Burke K and Ernzerhof M 1996 *Phys. Rev. Lett.* **77** 3865.
- [13] Terpstra H J, de Groot R A and Haas C 1995 *Phys. Rev. B* **52** 11690.
- [14] Yu R, Singh D and Krakauer H 1991 *Phys. Rev. B* **43** 6411.
- [15] Venkataraj S, Geurts J, Weis H, Kappertz O, Njoroge W K, Jayavel R and Wuttig M 2001 *J. Vac. Sci. Technol. A* **19** 2870.
- [16] Walsh A and Watson G W 2005 *J. Solid State Chemistry* **178** 1422.
- [17] Rubel O and Potvin A 2011 *AIP Conf. Proc.* **1368** 85.
- [18] Berashevich J, Semeniuk O, Rowlands J A and Reznik A 2012 *EPL* **99** 47005.
- [19] Thangaraju B and Kaliannann P 2000 *Semicond. Sci. Technol.* **15** 542.
- [20] Allen J P, Scanlon D O, Parker S C and Watson G W 2011 *J. Phys. Chem. C* **115** 19916.
- [21] Zacharia R, Ulbricht H, Hertel T 2004 *Phys. Rev. B* **69** 155406.
- [22] Berashevich J and Chakraborty T 2008 *J. Chem. Phys.* **128** 235101.
- [23] Togo A, Oba F, Tanaka I and Tatsumi K 2006 *Phys. Rev. B* **74** 195128.
- [24] NIST-JANAF Thermochemical Tables. <http://www.kinetics.nist.gov/janaf>
- [25] Van der Walle C G and Neugebauer J 2004 *J. Appl. Phys.* **95** 3851.
- [26] Wang L, Maxish T and Ceder G 2006 *Phys. Rev. B* **73** 195107.
- [27] Zheng J X, Ceder G, Maxisch T, Chim W K and Choi W K 2007 *Phys. Rev. B* **75** 104112.
- [28] Hammer B, Hansen L B and Norskov J K 1999 *Phys. Rev. B* **59** 7413.
- [29] Pople J A, Gordon M H, Fox D J, Raghavachari K and Curtiss L A 1989 *J. Chem. Phys.* **90** 5622.
- [30] Wasa K and Hayakawa S 1969 *Jap. J. Appl. Phys.* **8** 276.
- [31] Wolfe W L *Optical physics and engineering*, Plenum Press, New York, London, 1971; van der Broek J 1967 *Philips Res. Rep.* **22** 367.
- [32] Mahmood S A and Kabir M Z 2011 *J. Vac. Sci. Technol. A* **29** 031603.
- [33] Street R A 1990 *Appl. Phys. Lett.* **57** 1334.
- [34] Street R A, Ready S E, Lemmi F, Shah K S, Bennett P and Dmitriyev Y 1999 *J. Appl. Phys.* **86** 5.
- [35] Kasap S, Frey J B, Belev G, Tousignant O, Mani H, Laperriere L, Reznik A and Rowlands J A 2009 *Physica Status Solidi (b)* **246** 1794.
- [36] Kabir M Z, Kasap S O and J. A. Rowlands J A, in *Springer Handbook of Electronic and Photonic Materials*, edited by S. O. Kasap and PeterCapper (Springer, Heidelberg, Chap. 48, 2006).